and the contact lines' x values $x_l(t)$, $x_r(t)$ such that

$$\begin{aligned}
&-(p,\ \nabla\cdot\boldsymbol{\omega})_{\Omega_1}+\big(\eta_1(\nabla\mathbf{u}+(\nabla\mathbf{u})^T),\ \nabla\boldsymbol{\omega}\big)_{\Omega_1}\\
&+\frac{1}{Ca}(\partial_s\boldsymbol{\ell},\ \partial_s\boldsymbol{\omega})_{\Sigma_{3,l}}+\frac{1}{Ca}(\partial_s\mathbf{r},\ \partial_s\boldsymbol{\omega})_{\Sigma_{3,r}}-\frac{1}{Ca}(\nu,\ \nabla_s\cdot\boldsymbol{\omega})_{\Sigma_1} \qquad (3.86a)\\
&-\frac{\nu_l}{Ca}(\boldsymbol{\omega}\cdot\boldsymbol{\tau})\Big|_{\Lambda_l}+\frac{\gamma_1-\gamma_2}{Ca}\left((\boldsymbol{\omega}\cdot\boldsymbol{\tau})\Big|_{\Lambda_r}-(\boldsymbol{\omega}\cdot\boldsymbol{\tau})\Big|_{\Lambda_l}\right)=0,\quad\forall\boldsymbol{\omega}\in\mathbb{U}_2,
\end{aligned}$$

$$(\nabla\cdot\mathbf{u},\ \varphi)_{\Omega_1}=0,\quad\forall\varphi\in L^2(\Omega), \tag{3.86b}$$

$$\frac{l_s}{\mu_1}(\nabla_s\nu,\ \nabla_s g)_{\Sigma_1}+Ca\,(\nabla_s\cdot\mathbf{u},\ g)_{\Sigma_1}+\frac{1}{\mu_\Lambda}((\nu-\nu_l)g)\Big|_{\Lambda_l}+\frac{1}{\mu_\Lambda}(\nu,g)\Big|_{\Lambda_r}=0,$$
$$\forall g\in H^1([x_l,x_r]), \tag{3.86c}$$

$$-\int_{\Sigma_{2,l}}\frac{\kappa}{|\partial_x\mathbf{q}|}\frac{\partial y}{\partial t}\mathrm{d}l+(\mathbf{u}\cdot\boldsymbol{\tau})\Big|_{\Lambda_l}-\frac{1}{\mu_\Lambda Ca}(\nu-\nu_l)\Big|_{\Lambda_l}=0, \tag{3.86d}$$

$$\left(\dot{\boldsymbol{\ell}},\ \boldsymbol{\psi}_1\right)_{\Sigma_{3,l}}-(\mathbf{u},\ \boldsymbol{\psi}_1)_{\Sigma_{3,l}}=0,\quad\forall\boldsymbol{\psi}_1\in H^1(D)\times H_0^1(D), \tag{3.86e}$$

$$(\dot{\mathbf{r}},\ \boldsymbol{\psi}_2)_{\Sigma_{3,r}}-(\mathbf{u},\ \boldsymbol{\psi}_2)_{\Sigma_{3,r}}=0,\quad\forall\boldsymbol{\psi}_2\in H^1(D)\times H_0^1(D), \tag{3.86f}$$

$$\boldsymbol{\ell}(0,t)=(x_l(t),y(x_l(t),t)),\quad \mathbf{r}(0,t)=(x_r(t),y(x_r(t),t)). \tag{3.86g}$$

3.4.2 Numerical method

Similarly, we could propose a procedure to simulate the dynamics of the system, including two FEM schemes for the corresponding weak formulations (3.85a)-(3.85h) and (3.86a)-(3.86g).

The temporal discretization and the spatial discretization for the membrane in Sec. 3.3.2 are still available here by modifying $D_{\mathbf{q}}$ from $[-1,1]$ to $[0,B_x]$. We have two separated fluid-vacuum interfaces $\Sigma_{3,l}$ and $\Sigma_{3,r}$, but they share the same reference domain $D=[0,1]$. For simplicity, we set the same spatial discretization for these two fluid-vacuum interfaces as what we have done for the fluid-fluid interface Σ_3 in Sec. 3.3.2. We use the following finite-dimensional spaces to approximate V_y, $H^1_{0,r}(D^m_{\mathbf{q}})$, $H^1_0([0,x^m_l])$, $H^1([x^m_l,x^m_r])$, $H^1_{0,l}([x^m_r,B_x])$, respectively,

$$V^m_y:=\left\{f\in V^m: f(0)=-B_y\right\}, \tag{3.87a}$$

$$V_\kappa^m := \{f \in V^m : f(B_x) = 0\}, \tag{3.87b}$$

$$V_1^m := \Big\{g \in C([0, x_l^m]) : g|_{D^m_{\mathbf{q},j}} \in \mathcal{P}_2(D^m_{\mathbf{q},j}),\ \forall j = 1, 2, \cdots, j_l,\ g(0) = g(x_l^m) = 0\Big\}, \tag{3.87c}$$

$$V_2^m := \Big\{g \in C([x_l^m, x_r^m]) : g|_{D^m_{\mathbf{q},j}} \in \mathcal{P}_2(D^m_{\mathbf{q},j}),\ \forall j = j_l + 1, \cdots, j_r\Big\}, \tag{3.87d}$$

$$V_3^m := \Big\{g \in C([x_r^m, B_x]) : g|_{D^m_{\mathbf{q},j}} \in \mathcal{P}_2(D^m_{\mathbf{q},j}),\ \forall j = j_r + 1, \cdots, \mathcal{Q},\ g(x_r^m) = 0\Big\}, \tag{3.87e}$$

where V^m is defined in (3.58a). Besides, $H^1(D)$ can be approximated by W^h defined in (3.58e). $H_0^1(D)$ can be approximated by W_0^h defined in (3.58f). $H_{0,r}^1(D)$ can be approximated by

$$W_1^h := \big\{u \in W^h : u(1) = 0\big\}. \tag{3.88}$$

Using similar definitions in Sec. 3.3.2, the whole membrane Ξ at $t = t_m$ is approximated by Ξ^m. x_l^m and x_r^m separate Ξ^m into parts Σ_1^m, $\Sigma_{2,l}^m$, $\Sigma_{2,r}^m$, which numerically approximate Σ_1, $\Sigma_{2,l}$ and $\Sigma_{2,r}$, respectively, at $t = t_m$. For piecewise continuous functions u and v defined on the $D_{\mathbf{q}}^m$, the inner products on $\Sigma_{2,l}^m$ and $\Sigma_{2,r}^m$ can be approximated as

$$(u,\ v)_{\Sigma_{2,l}^m} := \sum_{j=1}^{j_l} |\partial_x \mathbf{q}^m|_j \int_{x_{j-1}^m}^{x_j^m} u(x)v(x)\mathrm{d}x, \tag{3.89a}$$

$$(u,\ v)_{\Sigma_{2,r}^m} := \sum_{j=j_r+1}^{\mathcal{Q}} |\partial_x \mathbf{q}^m|_j \int_{x_{j-1}^m}^{x_j^m} u(x)v(x)\mathrm{d}x. \tag{3.89b}$$

Let ν^m, ν_l^m be the numerical approximations to the membrane inner tension for Σ_1^m and $\Sigma_{2,l}^m$, respectively, at $t = t_m$.

Let $\Sigma_{3,l}^m := \boldsymbol{\ell}^m = (x_{\boldsymbol{\ell}}^m(\zeta), y_{\boldsymbol{\ell}}^m(\zeta)) \in W^h \times W_1^h$ and $\Sigma_{3,r}^m := \mathbf{r}^m = (x_{\mathbf{r}}^m(\zeta), y_{\mathbf{r}}^m(\zeta)) \in W^h \times W_1^h$ be the numerical approximations to the fluid-vacuum interfaces at $t = t_m$. For piecewise continuous functions u and v defined on D, the inner products on $\Sigma_{3,l}^m$

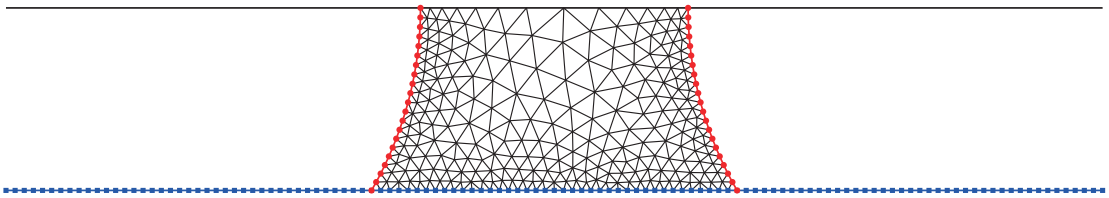

Figure 3.13: The initial fitted mesh used for the convergence test of the numerical method for bendotaxis. The red line with circle markers represents the fluid-vacuum interfaces. The blue line with square markers represents the lower membrane. The upper black line is the center line.

and $\Sigma_{3,r}^m$ can be approximated as

$$(u,\ v)_{\Sigma_{3,l}^m} := \sum_{j=1}^{\mathcal{R}} |\boldsymbol{\ell}^m(\zeta_j) - \boldsymbol{\ell}^m(\zeta_{j-1})| \int_{\zeta_{j-1}}^{\zeta_j} u(\zeta)v(\zeta)\mathrm{d}\zeta, \tag{3.90a}$$

$$(u,\ v)_{\Sigma_{3,r}^m} := \sum_{j=1}^{\mathcal{R}} |\mathbf{r}^m(\zeta_j) - \mathbf{r}^m(\zeta_{j-1})| \int_{\zeta_{j-1}}^{\zeta_j} u(\zeta)v(\zeta)\mathrm{d}\zeta, \tag{3.90b}$$

where $|\boldsymbol{\ell}^m(\zeta_j) - \boldsymbol{\ell}^m(\zeta_{j-1})|$ and $|\mathbf{r}^m(\zeta_j) - \mathbf{r}^m(\zeta_{j-1})|$ are the lengths of the line segments $[\boldsymbol{\ell}^m(\zeta_{j-1}), \boldsymbol{\ell}^m(\zeta_j)]$ and $[\mathbf{r}^m(\zeta_{j-1}), \mathbf{r}^m(\zeta_j)]$, respectively, for $j = 1, 2, \cdots, \mathcal{R}$.

We still denote $\mathbf{q}_j^m = (x_j^m, y^m(x_j^m)),\ j = 0, 1, \cdots, \mathcal{Q}$ as markers to represent the membrane Ξ^m. For fluid-vacuum interfaces $\Sigma_{3,l}^m$ and $\Sigma_{3,r}^m$, let $\boldsymbol{\ell}_j^m = \boldsymbol{\ell}^m(\zeta_j),\ j = 0, 1, \cdots, \mathcal{R}$ and $\mathbf{r}_j^m = \mathbf{r}^m(\zeta_j),\ j = 0, 1, \cdots, \mathcal{R}$ denote markers. Then, we have $\boldsymbol{\ell}_0^m = \mathbf{q}_{j_l}^m = (x_l^m, y^m(x_l^m))$ marking the left contact line Λ_l^m and $\mathbf{r}_0^m = \mathbf{q}_{j_r}^m = (x_r^m, y^m(x_r^m))$ marking the right contact line Λ_r^m.

Since Ω_2^m is a vacuum, a triangulation is only required for Ω_1^m. Let $\mathcal{T}^m := \bigcup_{j=1}^N \bar{o}_j^m$ be a triangulation of Ω_1^m at the time step $t = t_m$. The mesh contains J vertices denoted by $\{\mathbf{p}_k^m\}_{k=1}^J$. We use a fitted mesh (see Fig. 3.13) such that line segments of Σ_1^m, $\Sigma_{3,l}^m$ and $\Sigma_{3,r}^m$ are edges from $\mathcal{T}^m$, i.e., $\Sigma_1^m \cup \Sigma_{3,l}^m \cup \Sigma_{3,r}^m \subset \bigcup_{j=1}^N \partial o_j^m$. Compared to the triangulation for the first application, the number of triangles N and the number of vertices J are both independent of time here. It is because that no triangulation is reproduced in the numerical procedure introduced later.

We denote the corresponding finite element spaces for $\mathbb{U}_i$ $(i = 1, 2, 3)$ and $\mathbb{P}$ as

$\mathbb{U}_i^m$ $(i = 1, 2, 3)$ and $\mathbb{P}^m$, respectively. These finite element spaces are chosen to use the standard P2-(P1+P0) elements as

$$\mathbb{U}_1^m = [S_2^m]^2 \cap \mathbb{U}_1, \quad \mathbb{U}_2^m = [S_2^m]^2 \cap \mathbb{U}_2, \quad \mathbb{P}^m = (S_1^m + S_0^m) \cap \mathbb{P}, \tag{3.91a}$$

$$\mathbb{U}_3^m = \left\{ \boldsymbol{\omega} \in \mathbb{U}_1^m : \boldsymbol{\omega} \cdot \mathbf{n}^m = -\frac{1}{|\partial_x \mathbf{q}^m|} \frac{y^m - y^{m-1}}{\tau} \text{ on } \Sigma_1^m \right\}, \tag{3.91b}$$

where $|\partial_x \mathbf{q}^m| = \sqrt{1 + (\frac{\partial y^m}{\partial x})^2}$. These choices satisfy the inf-sup stability condition,

$$\inf_{\varphi \in \mathbb{P}^m} \sup_{0 \neq \boldsymbol{\omega} \in \mathbb{U}_i^m} \frac{(\varphi, \ \nabla \cdot \boldsymbol{\omega})_{\Omega_1^m}}{\|\varphi\|_0 \|\boldsymbol{\omega}\|_1} \geq C_0 > 0, \quad i = 1, 2, \tag{3.92}$$

where C_0 is a constant, and $\|\cdot\|_0$ and $\|\cdot\|_1$ denote the L^2 and H^1-norm on Ω_1^m, respectively.

The overall procedure of the numerical method is summarized as follows. Given the initial configuration of the system including $D_{\mathbf{q}}^0$, y^0 and κ^0 for the membrane Ξ^0, $\boldsymbol{\ell}^0$ and $\mathbf{r}^0$ for the fluid-vacuum interfaces $\Sigma_{3,l}^0$ and $\Sigma_{3,r}^0$, and $\mathcal{T}^0$ for the triangulation of Ω_1^0. Set $m = 0$ and then go through the following steps.

(1) Fix the current configuration of fluid-vacuum interfaces $\boldsymbol{\ell}^m$ and $\mathbf{r}^m$, and the positions of the contact lines x_l^m and x_r^m, based on the mesh $\mathcal{T}^m$, find the fluid velocity $\mathbf{u}^{m+\frac{1}{2}} \in \mathbb{U}_1^m$, the fluid pressure $p^{m+\frac{1}{2}} \in \mathbb{P}^m$, the membrane configuration $y^{m+\frac{1}{2}} \in V_y^m$, the curvature of the membrane $\kappa^{m+\frac{1}{2}} \in V_\kappa^m$, the inner tension of the membrane $\nu^{m+\frac{1}{2}} \in V_2^m$, and the constant inner tension $\nu_l^{m+\frac{1}{2}}$ for the membrane $\Sigma_{2,l}^{m+\frac{1}{2}}$ such that

$$\begin{aligned}
&-\Big(\overset{B'_{21}}{p^{m+\frac{1}{2}}}, \ \overset{B'_{22}}{\nabla \cdot \boldsymbol{\omega}^h}\Big)_{\Omega_1^m} + \Big(\overset{B_{11}}{\eta_1}(\overset{B_{12}}{\nabla \mathbf{u}^{m+\frac{1}{2}}} + \overset{B_{13}}{(\nabla \mathbf{u}^{m+\frac{1}{2}})^T}), \ \overset{B_{14}}{\nabla \boldsymbol{\omega}^h}\Big)_{\Omega_1^m} \\
&+ \frac{1}{Ca}\big(\partial_s \overset{I_{l1}}{\boldsymbol{\ell}^m}, \ \partial_s \boldsymbol{\omega}^h\big)_{\Sigma_{3,l}^m} + \frac{1}{Ca}\big(\partial_s \overset{I_{r1}}{\mathbf{r}^m}, \ \partial_s \boldsymbol{\omega}^h\big)_{\Sigma_{3,r}^m} \\
&+ \frac{1}{Ca}\left(\overset{M_{13}}{c_b \partial_s^m}\big(\overset{M_{14}}{\frac{\kappa^{m+\frac{1}{2}}}{|\partial_x \mathbf{q}^m|}}\big) - \overset{M_{11}}{\gamma^m \partial_s^m y^{m+\frac{1}{2}}}, \ \overset{M_{12}}{\partial_s^m}\left(|\partial_x \mathbf{q}^m| \boldsymbol{\omega}^h \cdot \mathbf{n}^m\right)\right)_{\Xi^m} \qquad (3.93a)\\
&+ \frac{3c_b}{2Ca}\big(\overset{M_{15}}{(\kappa^m)^2 \partial_s^m y^m}, \ \overset{M_{16}}{\partial_s^m}(|\partial_x \mathbf{q}^m| \boldsymbol{\omega}^h \cdot \mathbf{n}^m)\big)_{\Xi^m} - \frac{1}{Ca}\Big(\overset{G_{11}}{\nu^{m+\frac{1}{2}}}, \ \overset{G_{12}}{\nabla_s^m \cdot \boldsymbol{\omega}^h}\Big)_{\Sigma_1^m}
\end{aligned}$$

G31 G32 cl3 cl4

cl12 cl13 cl1 cl2

$|\partial_x q_h| w_1 = (\frac{\partial y}{\partial x} n|_{\Xi} + \tau)\cdot \omega$

CL1

$$
\begin{aligned}
&-\frac{1}{Ca}\left(\kappa^m \nu_l^{m+\frac{1}{2}},\ \boldsymbol{\omega}^h\cdot\mathbf{n}^m\right)_{\Sigma_{2,l}^m} - \frac{\nu_l^{m+\frac{1}{2}}}{Ca}(\boldsymbol{\omega}^h\cdot\boldsymbol{\tau}^m)\Big|_{\Lambda_l^m}\\
&+\frac{\gamma_1-\gamma_2}{Ca}\left((|\partial_x\mathbf{q}^m|\omega_1^h)\Big|_{\Lambda_r^m} - (|\partial_x\mathbf{q}^m|\omega_1^h)\Big|_{\Lambda_l^m}\right) = 0, \quad \forall\boldsymbol{\omega}^h = (\omega_1^h,\omega_2^h)\in\mathbb{U}_1^m,
\end{aligned}
$$

B21 B22

$$
\left(\nabla\cdot\mathbf{u}^{m+\frac{1}{2}},\ \varphi^h\right)_{\Omega_1^m} = 0, \quad \forall\varphi^h\in\mathbb{P}^m, \tag{3.93b}
$$

M22 M21 G2

M23

$$
\begin{aligned}
&\left(c_b\partial_s^m\Big(\frac{\kappa^{m+\frac{1}{2}}}{|\partial_x\mathbf{q}^m|}\Big) - \gamma_2\partial_s^m y^{m+\frac{1}{2}},\ \partial_s^m(|\partial_x\mathbf{q}^m|f_1^h)\right)_{\Sigma_{2,l}^m} - \left(\kappa^m\nu_l^{m+\frac{1}{2}},\ f_1^h\right)_{\Sigma_{2,l}^m}\\
&\quad+\frac{3c_b}{2}\left((\kappa^m)^2\partial_s^m y^m,\ \partial_s^m(|\partial_x\mathbf{q}^m|f_1^h)\right)_{\Sigma_{2,l}^m} = 0, \quad \forall f_1^h\in V_1^m,
\end{aligned}\tag{3.93c}
$$

M17 M18 M19

$$
\left(\frac{y^{m+\frac{1}{2}}-y^m}{\tau},\ f_2^h\right)_{\Sigma_1^m} + \left(|\partial_x\mathbf{q}^m|\mathbf{u}^{m+\frac{1}{2}}\cdot\mathbf{n}^m,\ f_2^h\right)_{\Sigma_1^m} = 0,\ \forall f_2^h\in V_2^m, \tag{3.93d}
$$

M32 M31

M33

$$
\begin{aligned}
&\left(c_b\partial_s^m\Big(\frac{\kappa^{m+\frac{1}{2}}}{|\partial_x\mathbf{q}^m|}\Big) - \gamma_2\partial_s^m y^{m+\frac{1}{2}},\ \partial_s^m(|\partial_x\mathbf{q}^m|f_3^h)\right)_{\Sigma_{2,r}^m}\\
&\quad+\frac{3c_b}{2}\left((\kappa^m)^2\partial_s^m y^m,\ \partial_s^m(|\partial_x\mathbf{q}^m|f_3^h)\right)_{\Sigma_{2,r}^m} = 0, \quad \forall f_3^h\in V_3^m,
\end{aligned}\tag{3.93e}
$$

M41 M42

$$
\left(\frac{\kappa^{m+\frac{1}{2}}}{|\partial_x\mathbf{q}^m|},\ \beta^h\right)_{\Xi^m} + \left(\partial_s^m y^{m+\frac{1}{2}},\ \partial_s^m\beta^h\right)_{\Xi^m} = 0, \quad \forall\beta^h\in V_\kappa^m, \tag{3.93f}
$$

G13 G14 G15

cl7

$$
\begin{aligned}
&\frac{l_s}{\mu_1}\left(\partial_s^m\nu^{m+\frac{1}{2}},\ \partial_s^m g^h\right)_{\Sigma_1^m} + Ca\left(\nabla_s^m\cdot\mathbf{u}^{m+\frac{1}{2}},\ g^h\right)_{\Sigma_1^m}\\
&\quad+\frac{1}{\mu_\Lambda}\left((\nu^{m+\frac{1}{2}}-\nu_l^{m+\frac{1}{2}})g^h\right)\Big|_{\Lambda_l^m} + \frac{1}{\mu_\Lambda}\left(\nu^{m+\frac{1}{2}}g^h\right)\Big|_{\Lambda_r^m} = 0, \quad \forall g^h\in V_2^m,
\end{aligned}\tag{3.93g}
$$

cl8 cl9 cl10 cl11

$$
-\int_{\Sigma_{2,l}^m}\frac{\kappa^m}{|\partial_x\mathbf{q}^m|}\frac{y^{m+\frac{1}{2}}-y^m}{\tau}\mathrm{d}l + (\mathbf{u}^{m+\frac{1}{2}}\cdot\boldsymbol{\tau}^m)\Big|_{\Lambda_l^m} - \underbrace{\frac{1}{\mu_\Lambda Ca}(\nu^{m+\frac{1}{2}}-\nu_l^{m+\frac{1}{2}})\Big|_{\Lambda_l^m}} = 0, \tag{3.93h}
$$

where $\gamma^m = \gamma_1\chi_{\Sigma_1^m} + \gamma_2\chi_{\Sigma_{2,l}^m} + \gamma_2\chi_{\Sigma_{2,r}^m}$.

(2) Due to the condition that the fluid-vacuum interfaces always stay on the membrane, update the y value of $\boldsymbol{\ell}^m(0)$ and $\mathbf{r}^m(0)$ as

$$
\boldsymbol{\ell}^{m+\frac{1}{2}}(\zeta) = \begin{cases}(x_l^m, y^{m+\frac{1}{2}}(x_l^m)), & \zeta = 0,\\ \boldsymbol{\ell}^m(\zeta), & 0<\zeta\le 1,\end{cases} \tag{3.94a}
$$

$$\mathbf{r}^{m+\frac{1}{2}}(\zeta) = \begin{cases} (x_r^m, y^{m+\frac{1}{2}}(x_r^m)), & \zeta = 0, \\ \mathbf{r}^m(\zeta), & 0 < \zeta \leq 1. \end{cases} \tag{3.94b}$$

Use the computed membrane configuration $y^{m+\frac{1}{2}}$ to update mesh from $\mathcal{T}^m$ to $\mathcal{T}^{m+\frac{1}{2}}$. Furthermore, we set $D_{\mathbf{q}}^{m+\frac{1}{2}}$ as $D_{\mathbf{q},j}^{m+\frac{1}{2}} = D_{\mathbf{q},j}^m$ for $j = 1, 2, \cdots, \mathcal{Q}$.

(3) Using the computed $y^{m+\frac{1}{2}}$ and $\kappa^{m+\frac{1}{2}}$, based on the mesh $\mathcal{T}^{m+\frac{1}{2}}$, find the fluid velocity $\mathbf{u}^{m+1} \in \mathbb{U}_3^{m+\frac{1}{2}}$, the fluid pressure $p^{m+1} \in \mathbb{P}^{m+\frac{1}{2}}$, the inner tension of the membrane $\nu^{m+1} \in V_2^{m+\frac{1}{2}}$, the constant inner tension ν_l^{m+1} for the membrane $\Sigma_{2,l}^{m+1}$, and the fluid-vacuum interfaces $\boldsymbol{\ell}^{m+1}$, $\mathbf{r}^{m+1} \in W^h \times W_1^h$ such that

$$-\left(\overset{\text{B}'_{21}}{p^{m+1}},\ \overset{\text{B}'_{22}}{\nabla \cdot \boldsymbol{\omega}^h}\right)_{\Omega_1^{m+\frac{1}{2}}} + \left(\overset{\text{B11}}{\eta_1(\nabla \mathbf{u}^{m+1}}\ \overset{\text{B12}}{+ (\nabla \mathbf{u}^{m+1})^T}\overset{\text{B13}}{)},\ \overset{\text{B14}}{\nabla \boldsymbol{\omega}^h}\right)_{\Omega_1^{m+\frac{1}{2}}} \tag{3.95a}$$
$$+ \frac{1}{Ca}\left(\overset{\text{Il1}}{\partial_s \boldsymbol{\ell}^{m+1}},\ \partial_s \boldsymbol{\omega}^h\right)_{\Sigma_{3,l}^{m+\frac{1}{2}}} + \frac{1}{Ca}\left(\overset{\text{Ir1}}{\partial_s \mathbf{r}^{m+1}},\ \partial_s \boldsymbol{\omega}^h\right)_{\Sigma_{3,r}^{m+\frac{1}{2}}}$$
$$- \frac{1}{Ca}\left(\overset{\text{G11}}{\nu^{m+1}},\ \overset{\text{G12}}{\nabla_s^{m+\frac{1}{2}} \cdot \boldsymbol{\omega}^h}\right)_{\Sigma_1^{m+\frac{1}{2}}} - \overset{\text{cl3}}{\frac{\nu_l^{m+1}}{Ca}}\overset{\text{cl4}}{(\boldsymbol{\omega}^h \cdot \boldsymbol{\tau}^{m+\frac{1}{2}})\Big|_{\Lambda_l^{m+\frac{1}{2}}}}$$
$$+ \frac{\gamma_1 - \gamma_2}{Ca}\left(\overset{\text{cl1}}{\left(\boldsymbol{\omega}^h \cdot \boldsymbol{\tau}^{m+\frac{1}{2}}\right)\Big|_{\Lambda_r^{m+\frac{1}{2}}}} - \overset{\text{cl2}}{\left(\boldsymbol{\omega}^h \cdot \boldsymbol{\tau}^{m+\frac{1}{2}}\right)\Big|_{\Lambda_l^{m+\frac{1}{2}}}}\right) = 0, \quad \forall \boldsymbol{\omega}^h \in \mathbb{U}_2^{m+\frac{1}{2}},$$

$$\left(\overset{\text{B21}}{\nabla \cdot \mathbf{u}^{m+1}},\ \overset{\text{B22}}{\varphi^h}\right)_{\Omega_1^{m+\frac{1}{2}}} = 0, \quad \forall \varphi^h \in \mathbb{P}^{m+\frac{1}{2}}, \tag{3.95b}$$

$$\frac{l_s}{\mu_1}\left(\overset{\text{G13}}{\partial_s^{m+\frac{1}{2}} \nu^{m+1}},\ \partial_s^{m+\frac{1}{2}} g^h\right)_{\Sigma_1^{m+\frac{1}{2}}} + Ca\left(\overset{\text{G14}}{\nabla_s^{m+\frac{1}{2}} \cdot \mathbf{u}^{m+1}},\ \overset{\text{G15}}{g^h}\right)_{\Sigma_1^{m+\frac{1}{2}}} \tag{3.95c}$$
$$+ \frac{1}{\mu_\Lambda}\left((\nu^{m+1} - \nu_l^{m+1})g^h\right)\Big|_{\Lambda_l^{m+\frac{1}{2}}} \overset{\text{cl7}}{+} \frac{1}{\mu_\Lambda}\left(\nu^{m+1} g^h\right)\Big|_{\Lambda_r^{m+\frac{1}{2}}} = 0, \quad \forall g^h \in V_2^{m+\frac{1}{2}},$$

$$- \overset{\text{cl8}\,*\,\frac{dy}{dt}}{\int_{\Sigma_{2,l}^{m+\frac{1}{2}}} \frac{\kappa^{m+\frac{1}{2}}}{|\partial_x \mathbf{q}^{m+\frac{1}{2}}|} \frac{y^{m+\frac{1}{2}} - y^m}{\tau} \mathrm{d}l} + \overset{\text{cl9}\ \ \text{cl10}}{(\mathbf{u}^{m+1} \cdot \boldsymbol{\tau}^{m+\frac{1}{2}})\Big|_{\Lambda_l^{m+\frac{1}{2}}}} \tag{3.95d}$$
$$- \frac{1}{\mu_\Lambda Ca}\overset{\text{cl11}}{(\nu^{m+1} - \nu_l^{m+1})}\Big|_{\Lambda_l^{m+\frac{1}{2}}} = 0,$$

$$\overset{\text{Il2}}{\left(\frac{\boldsymbol{\ell}^{m+1} - \boldsymbol{\ell}^{m+\frac{1}{2}}}{\tau},\ \boldsymbol{\psi}_1^h\right)_{\Sigma_{3,l}^{m+\frac{1}{2}}}} - \overset{\text{Il3}}{\left(\mathbf{u}^{m+1},\ \boldsymbol{\psi}_1^h\right)_{\Sigma_{3,l}^{m+\frac{1}{2}}}} = 0, \quad \forall \boldsymbol{\psi}_1^h \in W^h \times W_0^h, \tag{3.95e}$$

$$\overset{\text{Ir2}}{\left(\frac{\mathbf{r}^{m+1} - \mathbf{r}^{m+\frac{1}{2}}}{\tau},\ \boldsymbol{\psi}_2^h\right)_{\Sigma_{3,r}^{m+\frac{1}{2}}}} - \overset{\text{Ir3}}{\left(\mathbf{u}^{m+1},\ \boldsymbol{\psi}_2^h\right)_{\Sigma_{3,r}^{m+\frac{1}{2}}}} = 0, \quad \forall \boldsymbol{\psi}_2^h \in W^h \times W_0^h, \tag{3.95f}$$

$$\frac{y_{\boldsymbol{\ell}}^{m+1}(0) - y_{\boldsymbol{\ell}}^{m+\frac{1}{2}}(0)}{\tau} = \frac{\partial y^{m+\frac{1}{2}}}{\partial x}\Big|_{x=x_l^m} \frac{x_{\boldsymbol{\ell}}^{m+1}(0) - x_{\boldsymbol{\ell}}^{m+\frac{1}{2}}(0)}{\tau}, \tag{3.95g}$$

$$\frac{y_{\mathbf{r}}^{m+1}(0) - y_{\mathbf{r}}^{m+\frac{1}{2}}(0)}{\tau} = \frac{\partial y^{m+\frac{1}{2}}}{\partial x}\Big|_{x=x_r^m} \frac{x_{\mathbf{r}}^{m+1}(0) - x_{\mathbf{r}}^{m+\frac{1}{2}}(0)}{\tau}. \tag{3.95h}$$

(4) Update x_l^{m+1}, x_r^{m+1} with

$$x_l^{m+1} = x_{\boldsymbol{\ell}}^{m+1}(0), \quad x_r^{m+1} = x_{\mathbf{r}}^{m+1}(0). \tag{3.96}$$

Then we could update markers for the membrane $\mathbf{q}_j^{m+1}, j = 0, 1, \cdots, \mathcal{Q}$ as

$$\mathbf{q}_j^{m+1} = \begin{cases} (x_l^{m+1}, y_{\boldsymbol{\ell}}^{m+1}(0)), & j = j_l, \\ (x_r^{m+1}, y_{\mathbf{r}}^{m+1}(0)), & j = j_r, \\ (x_j^m, y^{m+\frac{1}{2}}(x_j^m)), & j = 0, 1, \cdots, \mathcal{Q} \text{ but } j \neq j_l, j_r. \end{cases} \tag{3.97}$$

(5) Fix the markers $\boldsymbol{\ell}_0^{m+1} = \mathbf{q}_{j_l}^{m+1}$, $\mathbf{r}_0^{m+1} = \mathbf{q}_{j_r}^{m+1}$ for the contact lines, according to the equal arclength, redistribute markers $\boldsymbol{\ell}_j^{m+1}$, $j = 1, 2, \cdots, \mathcal{R}-1$ for the fluid-vacuum interface $\Sigma_{3,l}^{m+1}$, markers $\mathbf{r}_j^{m+1}$, $j = 1, 2, \cdots, \mathcal{R}-1$ for the fluid-vacuum interface $\Sigma_{3,r}^{m+1}$, and markers $\mathbf{q}_j^{m+1}$, $j = j_l + 1, \cdots, j_r - 1$ for the membrane segment Σ_1^{m+1}. We compute the average arclength of Σ_1^{m+1}, and redistribute markers for $\Sigma_{2,l}^{m+1}$ and $\Sigma_{2,r}^{m+1}$ according to this average arclength. Due to the motion of the droplet towards the right end, We may add markers on $\Sigma_{2,l}^{m+1}$ or discard markers on $\Sigma_{2,r}^{m+1}$ to keep a good approximation. Once there is any addition or discard, we should update the values of j_l, j_r and $\mathcal{Q}$, but keep the values of $j_r - j_l$ and $\mathcal{R}$. After these redistribution, we obtain $D_{\mathbf{q}}^{m+1}$ and $y^{m+1} \in V_y^{m+1}$, and then compute the membrane curvature $\kappa^{m+1} \in V_\kappa^{m+1}$.

(6) Use the moving mesh method to generate the new fitted mesh $\mathcal{T}^{m+1}$ from $\mathcal{T}^m$. Then, go to step (1) with $m = m + 1$.